Transport of Indole-3-Butyric Acid and Indole-3-Acetic Acid in Arabidopsis Hypocotyls Using Stable Isotope Labeling[1][C][W][OA]

Xing Liu*, Lana Barkawi, Gary Gardner, and Jerry D. Cohen

Plant Biological Sciences Graduate Program, Department of Horticultural Science and Microbial and Plant Genomics Institute, University of Minnesota, St. Paul, Minnesota 55108

The polar transport of the natural auxins indole-3-butyric acid (IBA) and indole-3-acetic acid (IAA) has been described in Arabidopsis (*Arabidopsis thaliana*) hypocotyls using radioactive tracers. Because radioactive assays alone cannot distinguish IBA from its metabolites, the detected transport from applied [^{3}H]IBA may have resulted from the transport of IBA metabolites, including IAA. To test this hypothesis, we used a mass spectrometry-based method to quantify the transport of IBA in Arabidopsis hypocotyls by following the movement of [$^{13}C_1$]IBA and the [$^{13}C_1$]IAA derived from [$^{13}C_1$]IBA. We also assayed [$^{13}C_6$]IAA transport in a parallel control experiment. We found that the amount of transported [$^{13}C_1$]IBA was dramatically lower than [$^{13}C_6$]IAA, and the IBA transport was not reduced by the auxin transport inhibitor *N*-1-naphthylphthalamic acid. Significant amounts of the applied [$^{13}C_1$]IBA were converted to [$^{13}C_1$]IAA during transport, but [$^{13}C_1$]IBA transport was independent of IBA-to-IAA conversion. We also found that most of the [$^{13}C_1$]IBA was converted to ester-linked [$^{13}C_1$]IBA at the apical end of hypocotyls, and ester-linked [$^{13}C_1$]IBA was also found in the basal end at a level higher than free [$^{13}C_1$]IBA. In contrast, most of the [$^{13}C_6$]IAA was converted to amide-linked [$^{13}C_6$]IAA at the apical end of hypocotyls, but very little conjugated [$^{13}C_6$]IAA was found in the basal end. Our results demonstrate that the polar transport of IBA is much lower than IAA in Arabidopsis hypocotyls, and the transport mechanism is distinct from IAA transport. These experiments also establish a method for quantifying the movement of small molecules in plants using stable isotope labeling.

Indole-3-acetic acid (IAA), the most abundant form of the plant hormone auxin, is critical for plant growth and development. IAA levels are regulated in plants by multiple means, including biosynthesis of IAA through both Trp-dependent and Trp-independent pathways, conjugation of IAA via ester or amide bonds that can be hydrolyzed to release free IAA, polar transport of IAA over long distances, and degradation of IAA (for review, see Woodward and Bartel, 2005; Seidel et al., 2006).

Indole-3-butyric acid (IBA), which has had a long history of use as a synthetic auxin to promote root initiation, has been identified as an endogenous compound in a variety of plants (for review, see Ludwig-Müller, 2000), including Arabidopsis (*Arabidopsis thaliana*; Ludwig-Müller et al., 1993). IBA can be synthesized from IAA by a microsomal membrane preparation from maize (*Zea mays*) seedlings and by an enzyme preparation from Arabidopsis seedlings in the presence of acetyl-CoA and ATP (Ludwig-Müller et al., 1995a; Ludwig-Müller, 2007), but no mutants defective in this IAA-to-IBA conversion have been identified. Similar to IAA, IBA can be conjugated via both ester and amide bonds (for review, see Ludwig-Müller, 2000), and the major conjugate of exogenous IBA in Arabidopsis was identified as IBA-Glc (Ludwig-Müller and Epstein, 1993). Endogenous IBA-Glc was also found to be present in Arabidopsis at a high concentration, and this conjugation activity significantly affected plant development and tolerance to environmental stress (Tognetti et al., 2010). Importantly, IBA is converted to IAA via β-oxidation in a peroxisome-dependent manner (for review, see Woodward and Bartel, 2005; Strader and Bartel, 2011), and the IBA-derived IAA has been shown to be important for organ development in Arabidopsis (Strader et al., 2010, 2011).

Distinct transport streams occur in plants to transport IAA in a polar fashion. In hypocotyls, IAA moves basipetally from the shoot apex toward the roots. The machinery for IAA polar transport includes passive diffusion of protonated IAA, influx proteins (AUXIN RESISTANT1 [AUX1]/LIKE AUX1 [LAX]) that transport IAA into the cell, and efflux proteins (PIN-FORMED [PIN], ATP-BINDING CASSETTE B [ABCB]/PGP) that transport IAA out of the cell (for review, see Peer et al., 2011). The

[1] This work was supported by the National Science Foundation (grant nos. MCB0725149 and IOS–PGRP–0923960), the Minnesota Agricultural Experiment Station, and the Gordon and Margaret Bailey Endowment for Environmental Horticulture.

* Corresponding author; e-mail liuxx539@umn.edu.

The author responsible for distribution of materials integral to the findings presented in this article in accordance with the policy described in the Instructions for Authors (www.plantphysiol.org) is: Xing Liu (liuxx539@umn.edu).

[C] Some figures in this article are displayed in color online but in black and white in the print edition.

[W] The online version of this article contains Web-only data.

[OA] Open Access articles can be viewed online without a subscription.

www.plantphysiol.org/cgi/doi/10.1104/pp.111.191288

transport of IBA over long distances was suggested by an early study showing that IBA promotes the growth of *Avena* tissue distant from the application site, and the transport of IBA was found to be lower than IAA (Went and White, 1938). A study using intact pea (*Pisum sativum*) led to similar conclusions (Yang and Davies, 1999). The transport of IBA was also directly measured using radioactive IBA tracers. In midrib sections of Cleopatra mandarin (*Citrus reticulate* 'Blanco'), the basipetal transport of IBA was lower than IAA and was only about twice the acropetal transport (Epstein and Sagee, 1992). Using Arabidopsis inflorescence stems, Ludwig-Müller et al. (1995b) reported that [^{3}H]IBA was taken up to a greater extent than [^{14}C]IAA and was transported more rapidly. However, the acropetal transport of both [^{3}H]IBA and [^{14}C]IAA was greater than the basipetal transport in their system, suggesting that the measured transport was not polar (Rashotte et al., 2003). Also using radioactive IBA and IAA, Rashotte et al. (2003) performed a detailed study of auxin transport in different Arabidopsis tissues. They found basipetal transport of IAA but no transport of IBA in inflorescence stems, greater basipetal transport of IBA than IAA in hypocotyls, and both basipetal and acropetal transport of IAA and IBA in roots. Taken together, these reports suggest that similar to IAA, IBA can be transported over long distances in some plant tissues. However, knowing that IBA is converted to IAA (Strader et al., 2010) and that detecting radioactivity alone in plant tissues cannot distinguish [^{3}H]IBA from its metabolites (Fig. 1), it is possible that the transported compound was a metabolite of [^{3}H]IBA, such as [^{3}H]IAA. Consistent with this hypothesis, using HPLC to distinguish [^{3}H]IBA from [^{3}H]IAA, Ruzicka et al. (2010) found that after [^{3}H]IBA was applied to Arabidopsis root columella cells, most of the [^{3}H]IBA was converted to [^{3}H]IAA when the radioactivity reached the region up to 4 mm above the root tip, which suggests that only IAA derived from IBA can be transported to areas distant from the IBA application site. To better distinguish IBA and IAA derived from IBA, we decided to use gas chromatography-mass spectrometry (GC-MS) to analyze the transported compounds after the application of stable isotope-labeled IBA, where both IAA and IBA from the same plant sample can be measured simultaneously (Sutter and Cohen, 1992; Barkawi et al., 2008). In preliminary studies (Supplemental Fig. S1), we found that when [$^{13}C_8$,$^{15}N_1$]IBA was applied to maize coleoptile sections, a significant portion of the stable-labeled compounds detected in the agar receiver block was [$^{13}C_8$,$^{15}N_1$]IAA derived from [$^{13}C_8$,$^{15}N_1$]IBA, and *N*-1-naphthylphthalamic acid (NPA) inhibited the movement of [$^{13}C_8$,$^{15}N_1$]IAA into the receiver. We also found that a very small amount of [$^{13}C_8$,$^{15}N_1$]IBA moved basipetally in a polar fashion, but this movement was not inhibited by NPA. These results suggest that by using specific labeled compounds and GC-MS analysis, the movement and metabolic changes of the labeled compounds can be accurately measured.

To evaluate the role of IBA-to-IAA conversion and IBA metabolism in the transport of IBA in Arabidopsis hypocotyls, we applied [$^{13}C_1$]IBA instead of radioactive tracers in our established system for polar auxin transport measurement in Arabidopsis hypocotyls (Liu et al., 2011), and we quantified the transported compounds by GC-MS/MS, using [$^{13}C_8$,$^{15}N_1$]IBA and [$^{2}H_4$]IAA as internal standards. As a comparison, we used the same approach and quantified the transport of [$^{13}C_6$]IAA in Arabidopsis hypocotyls. We found that a significant portion of [$^{13}C_6$]IAA taken up by Arabidopsis hypocotyls moved basipetally and that the majority of the transported [$^{13}C_6$]IAA remained as free [$^{13}C_6$]IAA. In contrast, a large portion of [$^{13}C_1$]IBA was converted to [$^{13}C_1$]IAA and ester-linked [$^{13}C_1$]IBA during the transport period, and the proportion of the applied [$^{13}C_1$]IBA transported basipetally was much lower than the proportion of applied [$^{13}C_6$]IAA transported basipetally, suggesting that long-distance transport of IBA has a much smaller effect on IBA pools than transport of IAA has on IAA pools.

RESULTS

Absolute Quantification of Auxin Transport Using Stable Isotope-Labeled Tracers

We previously established a sensitive [^{3}H]IAA transport assay with low background noise to measure

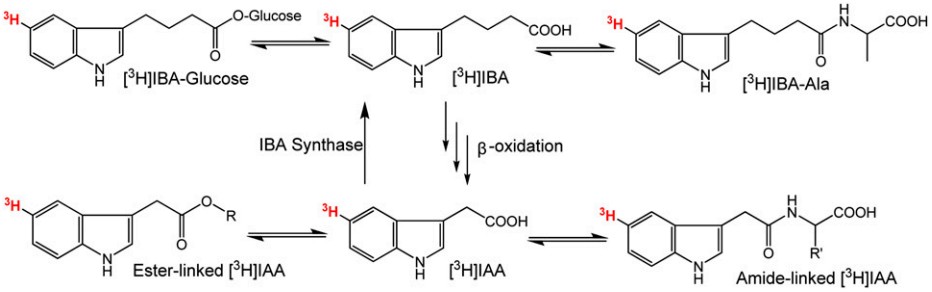

Figure 1. Possible metabolic pathways of [^{3}H]IBA and [^{3}H]IAA (adapted from Woodward and Bartel, 2005). [^{3}H]IBA can be converted to [^{3}H]IAA via β-oxidation through multiple steps, and [^{3}H]IBA can also be synthesized from [^{3}H]IAA via IBA synthase. Both [^{3}H]IBA and [^{3}H]IAA can be converted to ester-linked and amide-linked conjugated forms. [See online article for color version of this figure.]

the transport of IAA in Arabidopsis hypocotyls (Liu et al., 2011). To achieve better compound identification, isotope analysis, and the quantification of transported IAA and IBA, we modified the assay and changed from a radioactive auxin tracer to a stable isotope system using either [$^{13}C_6$]IAA or [$^{13}C_1$]IBA (Fig. 2A). In order to recover a sufficient quantity of transported [$^{13}C_6$]IAA and [$^{13}C_1$]IBA for GC-MS/MS analysis, we applied stable-labeled auxin in the donor agar block at 10^{-5} M, a concentration that was reported to yield maximal basipetal auxin transport (Rashotte et al., 2003). After a 5-h transport period, auxins were determined in pools of lower hypocotyl sections and receivers. Five plants were needed for facile detection of [$^{13}C_6$]IAA, while 20 plants were needed for detection of [$^{13}C_1$]IBA and [$^{13}C_1$]IAA derived from [$^{13}C_1$]IBA. As shown in Figure 2B, when [$^{13}C_6$]IAA was added in the donor agar block, unlabeled endogenous IAA, [$^{13}C_6$]IAA tracer, and the [$^{2}H_4$]IAA internal standard were detected separately; thus, the [$^{13}C_6$]IAA tracer could be distinguished from endogenous IAA, and the amount of [$^{13}C_6$]IAA could be quantified based on the [$^{2}H_4$]IAA internal standard. Potential [$^{13}C_6$]IBA derived from [$^{13}C_6$]IAA was also monitored but was not detected, which may be due to a low rate of conversion of [$^{13}C_6$]IBA that may require more tissue for detection. Similarly, when [$^{13}C_1$]IBA was added in the donor agar block (Fig. 2C), both IAA and IBA were monitored, and their retention times on GC were about 1 min apart. Therefore, unlabeled endogenous IBA and IAA, [$^{13}C_1$]IBA tracer and its metabolic product [$^{13}C_1$]IAA, and [$^{13}C_8$,$^{15}N_1$]IBA and [$^{2}H_4$]IAA internal standards were all detected separately, and the amounts of [$^{13}C_1$]IBA and [$^{13}C_1$]IAA could be quantified based on the internal standards. Clearly, using stable isotope-labeled auxins and GC-MS/MS, we are able to quantify the absolute amount of both endogenous and applied IAA and IBA transported.

Transport of Free [$^{13}C_6$]IAA and [$^{13}C_1$]IBA in Arabidopsis Hypocotyls

When [$^{13}C_6$]IAA was supplied in donor agar blocks and incubated with Arabidopsis hypocotyl sections for 5 h, 42 pg of [$^{13}C_6$]IAA was detected per upper section (Fig. 3A) and 17 pg of [$^{13}C_6$]IAA was detected per lower section and receiver (Fig. 3B). Therefore, about 29% of the [$^{13}C_6$]IAA in the hypocotyl section was transported basipetally to the lower section and receiver (Fig. 3C). (The percentage transport is defined for [$^{13}C_6$]IAA as the amount of free auxin in the lower section and receiver [17 pg; Fig. 3B] divided by the sum of free auxin in the upper plus lower sections and the receiver [59 pg] and, similarly, for [$^{13}C_1$]IBA, 0.26 pg in the lower section and receiver divided by 42.26 pg in the upper plus lower sections and the receiver.) When 10^{-5} M of the auxin transport inhibitor NPA was added in the receiver block, the level of [$^{13}C_6$]IAA per lower section and receiver was reduced to 1 pg without a concomitant reduction in the level of [$^{13}C_6$]IAA per upper section (Fig. 3, A and B). This result suggests that NPA diffused into the hypocotyl tissue from the receiver and thus dramatically inhibited the polar transport of [$^{13}C_6$]IAA into the lower hypocotyl section without resulting in an overaccumulation of [$^{13}C_6$]IAA in the upper hypocotyl section. In the acropetal control, each upper section contained 85 pg of [$^{13}C_6$]IAA and each lower section and receiver contained only 1 pg of [$^{13}C_6$]IAA, suggesting a very low background level of diffusion in this transport assay.

In a parallel experiment, [$^{13}C_1$]IBA was supplied in donor agar blocks to quantify the transport of IBA. After a 5-h transport period, 42 pg of [$^{13}C_1$]IBA was detected per upper section (Fig. 3D), which was similar to the amount of [$^{13}C_6$]IAA transported (described above). However, only 0.26 pg of [$^{13}C_1$]IBA was found per lower section and receiver (Fig. 3E); therefore, only 0.62% of the [$^{13}C_1$]IBA in the hypocotyl section was transported basipetally to the lower section and receiver (Fig. 3F). (See above for percentage transport definition.) Importantly, [$^{13}C_1$]IAA derived from [$^{13}C_1$]IBA was also detected in both sections, and 0.2 pg of [$^{13}C_1$]IAA was found per upper section while 0.34 pg of [$^{13}C_1$]IAA was found per lower section and receiver (Fig. 3, G and H). Interestingly, adding NPA in the receiver did not change the level of [$^{13}C_1$]IBA in either section (Fig. 3, D and E), but NPA reduced the level of [$^{13}C_1$]IAA per lower section and receiver to 0.03 pg (Fig. 3H), suggesting that NPA inhibits the transport of [$^{13}C_1$]IAA derived from [$^{13}C_1$]IBA but not the transport of [$^{13}C_1$]IBA itself. In the acropetal control, [$^{13}C_1$]IBA and [$^{13}C_1$]IAA were almost undetectable in the lower section and receiver, and the percentage transport of [$^{13}C_1$]IBA was significantly lower than that found with the other two experimental groups ($P < 0.01$; Fig. 3F). These results suggest that the transport of free IBA is much lower than the transport of free IAA in Arabidopsis hypocotyls (less than 1% compared with 29%) and show that IAA synthesized from IBA also enters the IAA transport stream.

Because the transport of [$^{13}C_1$]IBA was very low and was not inhibited by NPA, it is possible that IBA was only transported in the phloem. To test this hypothesis, we quantified the transport of [$^{13}C_6$]IAA and [$^{13}C_1$]IBA in the *nakr1* mutant, which was reported to be defective in phloem function but displays normal seedling growth (Tian et al., 2010). As shown in Figure 4, the transport of [$^{13}C_6$]IAA and [$^{13}C_1$]IBA in the *nakr1* mutant was the same as that in wild-type plants, indicating that the aspect of phloem transport blocked in *nakr1* plants does not play an essential role in the transport of IAA or IBA.

Transport of Free [$^{13}C_6$]IAA and [$^{13}C_1$]IBA in *ibr1 ibr3 ibr10* Arabidopsis Hypocotyls

Because IAA can be converted to IBA and IBA can be converted back to IAA, each via specific metabolic pathways in vivo (Fig. 1), it is possible that the transport of IBA may be dependent on these interconversions. To

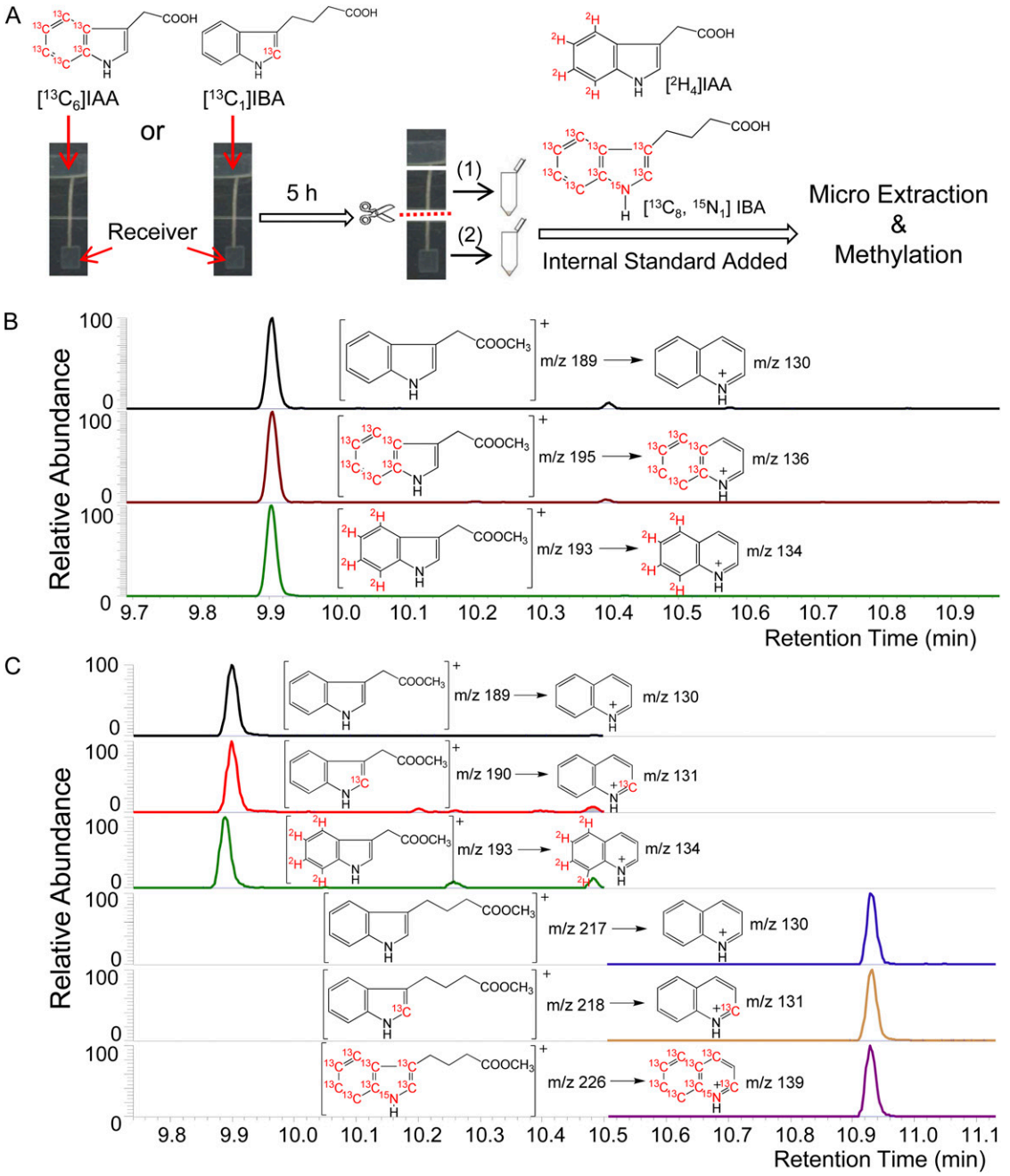

Figure 2. Summary of the experimental procedures. SRM-MS was used to detect molecular ion-to-major fragment ion transitions produced by methylated IAA and IBA. The major fragment ion for both 3-substituted indoles involves a ring expansion to form the relatively stable quinolinium ion in high yield (Marx and Djerassi, 1968). A, Donor agar blocks containing 10^{-5} M [$^{13}C_6$]IAA or [$^{13}C_1$]IBA were placed on top of 6-mm Arabidopsis hypocotyl sections. After 5 h, the hypocotyl sections were cut horizontally into halves. Samples containing upper half-hypocotyl sections (1) and containing lower half-hypocotyl sections plus receivers (2) were collected and extracted with known amounts of [$^{2}H_4$]IAA and [$^{13}C_8$,$^{15}N_1$]IBA added as internal standards. B, Chromatographic results of samples labeled by [$^{13}C_6$]IAA. From top to bottom: unlabeled endogenous IAA, [$^{13}C_6$]IAA from donor block, and [$^{2}H_4$]IAA internal standard. C, Chromatographic results of samples labeled by [$^{13}C_1$]IBA. From top to bottom: unlabeled endogenous IAA, [$^{13}C_1$]IAA derived from [$^{13}C_1$]IBA, [$^{2}H_4$]IAA internal standard, unlabeled endogenous IBA, [$^{13}C_1$]IBA from donor block, and [$^{13}C_8$,$^{15}N_1$]IBA internal standard. [See online article for color version of this figure.]

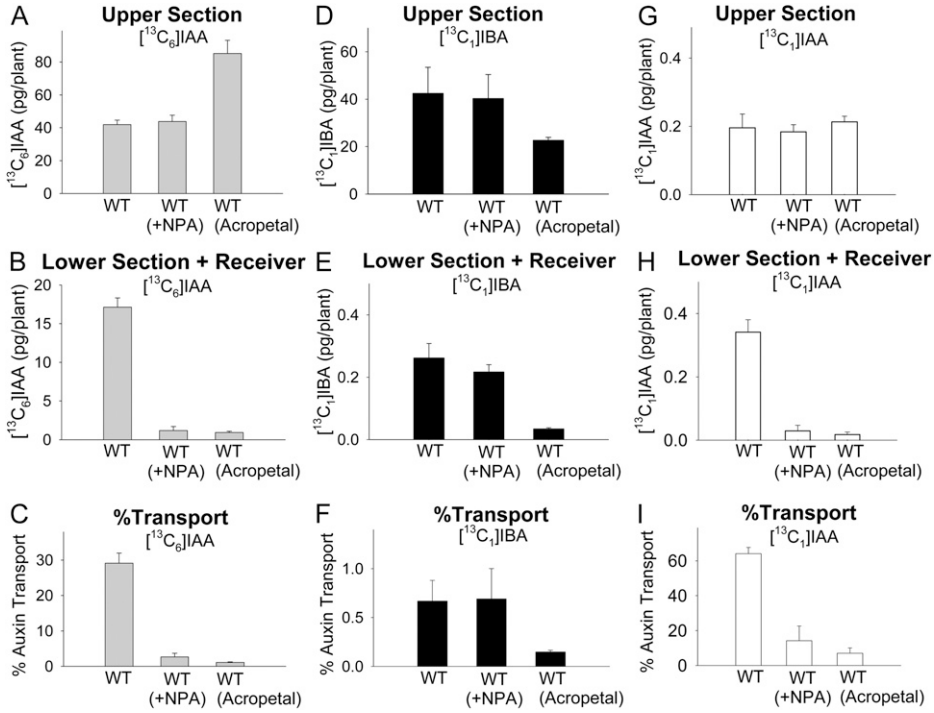

Figure 3. Polar auxin transport and quantification of free [$^{13}C_6$]IAA, [$^{13}C_1$]IBA, and [$^{13}C_1$]IAA derived from [$^{13}C_1$]IBA in wild-type Arabidopsis hypocotyls after 5-h transport periods. WT, Wild type; WT (+NPA), 10^{-5} M NPA was added in receivers; WT (Acropetal), control with reversed orientation of hypocotyl sections. Error bars represent SE. A, Amounts of [$^{13}C_6$]IAA in the upper half-hypocotyl sections. B, Amounts of [$^{13}C_6$]IAA transported into the lower half-hypocotyl sections and receiver. C, Percentage transport of [$^{13}C_6$]IAA, calculated as values in B divided by the sum of values in A and B. Transport of [$^{13}C_6$]IAA was dramatically reduced by NPA ($P < 0.001$, $n = 3$, Student's t test), which was similar to the acropetal control. D, Amounts of [$^{13}C_1$]IBA in the upper half-hypocotyl sections. E, Amounts of [$^{13}C_1$]IBA transported into the lower half-hypocotyl sections and receiver. F, Percentage transport of [$^{13}C_1$]IBA, calculated as values in E divided by the sum of values in D and E. Transport of [$^{13}C_1$]IBA transport in WT (+NPA) was not different from that in the wild type but was significantly higher than in WT (Acropetal) ($P < 0.01$, $n = 3$, Student's t test). G, Amounts of [$^{13}C_1$]IAA derived from [$^{13}C_1$]IBA in the upper half-hypocotyl sections. H, Amounts of [$^{13}C_1$]IAA derived from [$^{13}C_1$]IBA transported into the lower half-hypocotyl sections and receiver. [$^{13}C_1$]IAA was detected in the wild type, and the amounts were significantly reduced in WT (+NPA) and WT (Acropetal) ($P < 0.002$, $n = 3$, Student's t test). I, Percentage transport of [$^{13}C_1$]IAA, calculated as values in H divided by the sum of values in G and H.

test this possibility, we quantified the transport of [$^{13}C_6$]IAA and [$^{13}C_1$]IBA in the *ibr1 ibr3 ibr10* triple mutant, in which the capacity for the conversion of IBA to IAA is dramatically reduced (Strader et al., 2010). As shown in Figure 5H, in the lower section and receiver, the level of [$^{13}C_1$]IAA derived from [$^{13}C_1$]IBA was significantly lower in *ibr1 ibr3 ibr10* than in the wild type ($P < 0.002$), but there was no significant difference in the level of [$^{13}C_1$]IBA transported (Fig. 5E). Therefore, the transport of [$^{13}C_1$]IBA was not affected in the *ibr1 ibr3 ibr10* mutant (Fig. 5F), suggesting that the measured transport of [$^{13}C_1$]IBA in the wild type does not depend on the conversion between IBA and IAA. On the other hand, the transport of [$^{13}C_6$]IAA was significantly reduced in *ibr1 ibr3 ibr10* ($P < 0.05$; Fig. 5C), and the amount of [$^{13}C_6$]IAA taken up by *ibr1 ibr3 ibr10* plants (the sum of values in Fig. 5, A and B) was significantly lower than the wild type ($P < 0.002$, $n = 3$, Student's t test), suggesting that disruption of IBR1, IBR3, and IBR10 affects aspects of IAA distribution.

Transport and Metabolism of [$^{13}C_6$]IAA and [$^{13}C_1$]IBA in Arabidopsis Hypocotyls

Free IAA and IBA can be released from their conjugated forms via chemical hydrolysis: weak base hydrolysis breaks the ester linkage (Baldi et al., 1989), while strong base hydrolysis breaks both ester and amide linkages (Bialek and Cohen, 1989). Using different strengths of base hydrolysis, we quantified the level of [$^{13}C_6$]IAA and [$^{13}C_1$]IBA released from their ester- and amide-linked conjugates, in both upper section and lower section plus receiver, after a 5-h transport period. When [$^{13}C_6$]IAA was supplied in the donor agar block, each upper section of the basipetal group contained 35 pg of [$^{13}C_6$]IAA, 17 pg of IAA equivalents ester-linked [$^{13}C_6$]IAA, and 37 pg of IAA equivalents amide-linked [$^{13}C_6$]IAA (Fig. 6A); each lower section and receiver contained 22 pg of [$^{13}C_6$]IAA and a very small amount of conjugated [$^{13}C_6$]IAA (Fig. 6B). Interestingly, when NPA was added in the receiver, the level of [$^{13}C_6$]IAA and ester-linked [$^{13}C_6$]

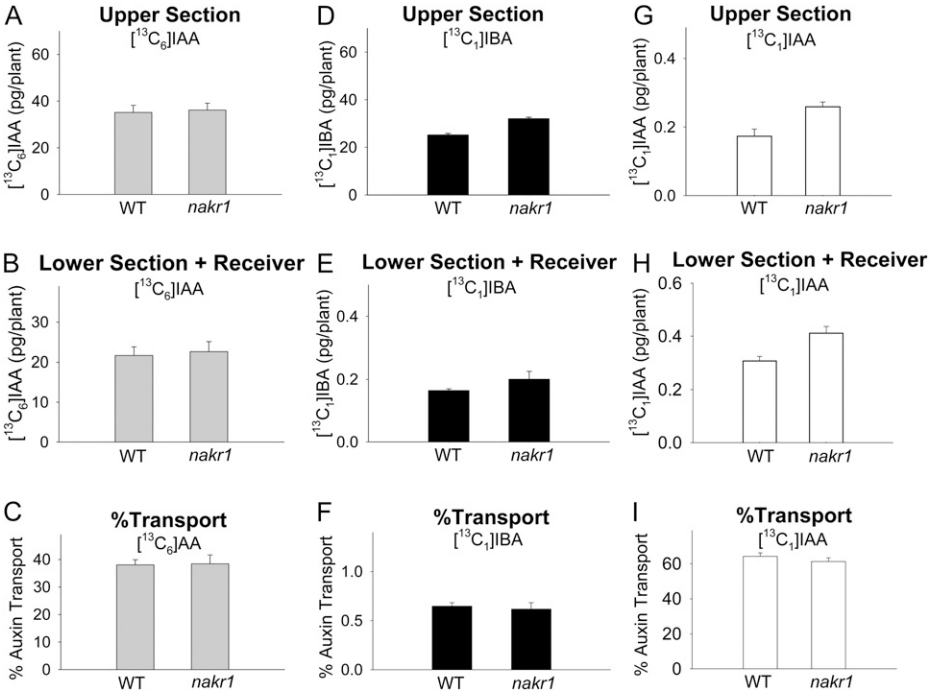

Figure 4. Polar auxin transport and quantification of free [$^{13}C_6$]IAA, [$^{13}C_1$]IBA, and [$^{13}C_1$]IAA derived from [$^{13}C_1$]IBA in wild-type and *nakr1* mutant Arabidopsis hypocotyls after 5-h transport periods. WT, Wild type. Error bars represent SE. A, Amounts of [$^{13}C_6$]IAA in the upper half-hypocotyl sections. B, Amounts of [$^{13}C_6$]IAA transported into the lower half-hypocotyl sections and receiver. C, Percentage transport of [$^{13}C_6$]IAA, calculated as values in B divided by the sum of values in A and B. Transport of [$^{13}C_6$]IAA in the *nakr1* mutant was not different from that in the wild type. D, Amounts of [$^{13}C_1$]IBA in the upper half-hypocotyl sections. E, Amounts of [$^{13}C_1$]IBA transported into the lower half-hypocotyl sections and receiver. F, Percentage transport of [$^{13}C_1$]IBA, calculated as values in E, divided by the sum of values in D and E. Transport of [$^{13}C_1$]IBA in the *nakr1* mutant was not different from that in the wild type. G, Amounts of [$^{13}C_1$]IAA derived from [$^{13}C_1$]IBA in the upper half-hypocotyl sections. H, Amounts of [$^{13}C_1$]IAA derived from [$^{13}C_1$]IBA transported into the lower half-hypocotyl sections and receiver. I, Percentage transport of [$^{13}C_1$]IAA, calculated as values in H divided by the sum of values in G and H.

IAA was not changed per upper section, but the amount of amide-linked [$^{13}C_6$]IAA was significantly increased ($P < 0.05$; Fig. 6A) and reached 208 pg per plant. Similarly, in the upper section from the acropetal control, the level of amide-linked [$^{13}C_6$]IAA was significantly higher than in the basipetal group. On the other hand, a very small amount of free and conjugated [$^{13}C_6$]IAA was detected in the lower section and receiver of the NPA and acropetal groups (Fig. 6B). These results confirm that amide-linked IAA is the major conjugate derived from exogenous IAA (Staswick et al., 2005; for review, see Slovin et al., 1999) and show that free IAA is the primary form of transported IAA.

When [$^{13}C_1$]IBA was supplied in the donor agar block, each upper section of the basipetal group contained 25 pg of [$^{13}C_1$]IBA, 458 pg of IBA equivalents ester-linked [$^{13}C_1$]IBA, 27 pg of IBA equivalents amide-linked [$^{13}C_1$]IBA, and 0.17 pg of [$^{13}C_1$]IAA (Fig. 6C). A similar pattern of these components was also found in the NPA group (Fig. 6C). In each lower section and receiver of the basipetal group, there was 0.16 pg of [$^{13}C_1$]IBA, 0.52 pg of ester-linked [$^{13}C_1$]IBA, 0.09 pg of amide-linked [$^{13}C_1$]IBA, and 0.31 pg of [$^{13}C_1$]IAA (Fig. 6D); adding NPA in the receiver did not change the levels of free and conjugated [$^{13}C_1$]IBA significantly but reduced the level of [$^{13}C_1$]IAA to 0.01 pg per plant (Fig. 6D). These results suggest that a large portion of exogenous IBA is converted to ester-linked IBA and that an extremely small portion of free and/or ester-linked IBA is transported to the lower hypocotyl sections.

DISCUSSION

The aim of this study was to evaluate the transport of IBA and IAA in Arabidopsis hypocotyls using methods that provide accurate compound identification and absolute quantification. To our knowledge, this is the first time that the polar transport of auxins and their metabolites has been measured using the stable isotope labeling approach. Rashotte et al. (2003) found that when various concentrations of [^{3}H]IAA or [^{3}H]IBA were applied in an agar donor block, both [^{3}H]IAA and [^{3}H]IBA moved basipetally in Arabidopsis hypocotyls, and the transport of [^{3}H]IBA was higher than the transport of [^{3}H]IAA. They argued that the conversion from [^{3}H]IBA to [^{3}H]IAA did not contrib-

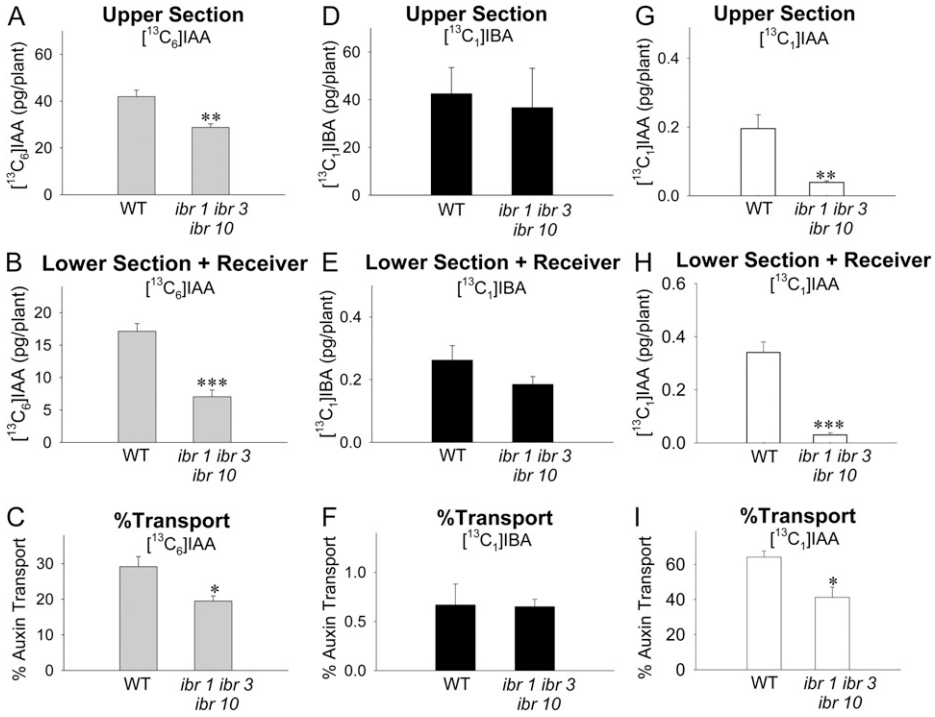

Figure 5. Polar auxin transport and quantification of free [$^{13}C_6$]IAA, [$^{13}C_1$]IBA, and [$^{13}C_1$]IAA derived from [$^{13}C_1$]IBA in wild-type and *ibr1 ibr3 ibr10* mutant Arabidopsis hypocotyls after 5-h transport periods. WT, Wild type. Error bars represent SE. The +NPA and acropetal controls were also performed using *ibr1 ibr3 ib10* mutant plants, and the results were similar to the wild-type results shown in Figure 3. A, Amounts of [$^{13}C_6$]IAA in the upper half-hypocotyl sections. B, Amounts of [$^{13}C_6$]IAA transported into the lower half-hypocotyl sections and receiver. C, Percentage transport of [$^{13}C_6$]IAA, calculated as values in B divided by the sum of values in A and B. Transport of [$^{13}C_6$]IAA in the *ibr1 ibr3 ibr10* mutant was significantly lower than in the wild type. D, Amounts of [$^{13}C_1$]IBA in the upper half-hypocotyl sections. E, Amounts of [$^{13}C_1$]IBA transported into the lower half-hypocotyl sections and receiver. F, Percentage transport of [$^{13}C_1$]IBA, calculated as values in E divided by the sum of values in D and E. Transport of [$^{13}C_1$]IBA in the *ibr1 ibr3 ibr10* mutant was not different from the wild type. G, Amounts of [$^{13}C_1$]IAA derived from [$^{13}C_1$]IBA in the upper half-hypocotyl sections. H, Amounts of [$^{13}C_1$]IAA derived from [$^{13}C_1$]IBA transported into the lower half-hypocotyl sections and receiver. The amount of [$^{13}C_1$]IAA was significantly reduced in the *ibr1 ibr3 ibr10* mutant compared with the wild type. I, Percentage transport of [$^{13}C_1$]IAA, calculated as values in H divided by the sum of values in G and H. Student's *t* test ($n = 3$): * $P < 0.05$, ** $P < 0.02$, *** $P < 0.002$.

ute to the measured transport of [^{3}H]IBA, because no transport of [^{3}H]IBA was detected in the Arabidopsis inflorescence axis where basipetal transport of [^{3}H]IAA occurred and because no [^{3}H]IAA was detected using thin-layer chromatography after incubating Arabidopsis seedlings with [^{3}H]IBA. However, the metabolism of [^{3}H]IBA in the inflorescence might be different from that in hypocotyls, and the detection of radioactivity on a thin-layer chromatography plate does not provide a sensitive and precise measurement of [^{3}H]IBA and its metabolites. Indeed, in a more recent study using GC-MS for IAA and IBA quantification, Strader et al. (2010) found a significant amount of stable-labeled IAA derived from stable-labeled IBA in Arabidopsis seedlings. Using HPLC to separate [^{3}H]IAA from [^{3}H]IBA, Ruzicka et al. (2010) showed that although [^{3}H]IBA was transported out of the root apex in an ABCG37-dependent manner, most of the [^{3}H]IBA was converted to [^{3}H]IAA in root tissue above the apex, suggesting that IAA, but not IBA, is the compound responsible for the long-distance transport of radioactivity derived from [^{3}H]IBA. However, detection of radioactivity after HPLC does not provide quantitative information about the transported compounds, so it is difficult to evaluate the contribution of the transport activity. Also, HPLC retention time alone does not provide precise compound identification. Therefore, we decided to replace the radioactive tracers with stable isotope-labeled IBA and IAA, which can be distinguished from the endogenous compounds by GC-MS/MS based on their mass differences (Fig. 2), and we can quantify the amount of transported compounds using differently labeled internal standards and the isotope dilution technique.

Rashotte et al. (2003) found that when concentrations of IAA and IBA in the donor agar block were increased from 10^{-7} M to 2×10^{-5} M, the transport of [^{3}H]IAA and [^{3}H]IBA in Arabidopsis hypocotyls was also increased and saturated at high concentrations. Because sufficient amounts of transported [$^{13}C_6$]IAA and [$^{13}C_1$]IBA are required for GC-MS analysis but high concentrations of auxin can significantly induce auxin conjugation activities (Sudi, 1966; Li et al., 1999),

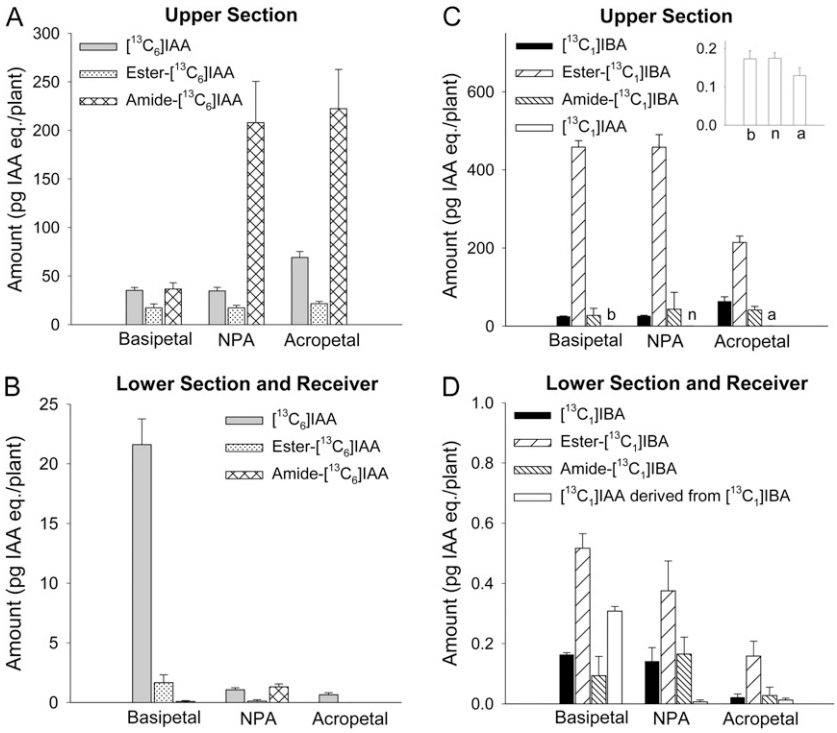

Figure 6. Quantification of free [$^{13}C_6$]IAA, free [$^{13}C_1$]IBA, and the ester- or amide-linked conjugates they formed in wild-type Arabidopsis hypocotyls after 5-h transport periods. A, Amounts of free, ester-linked, and amide-linked [$^{13}C_6$]IAA in the upper half-hypocotyl sections. The levels of amide-linked [$^{13}C_6$]IAA in NPA and acropetal groups were significantly higher than in the basipetal group ($P < 0.05$, $n = 3$, Student's t test). B, Amounts of free, ester-linked, and amide-linked [$^{13}C_6$]IAA in the lower half-hypocotyl sections and receivers. Free [$^{13}C_6$]IAA was the dominant form of transported auxin. C, Amounts of free, ester-linked, and amide-linked [$^{13}C_1$]IBA and [$^{13}C_1$]IAA derived from [$^{13}C_1$]IBA in the upper half-hypocotyl sections. The lettered bars are shown in the inset graph using an expanded scale for better visualization of the values. Ester-linked [$^{13}C_1$]IBA was the dominant metabolic product of [$^{13}C_1$]IBA. D, Amounts of free, ester-linked, and amide-linked [$^{13}C_1$]IBA and [$^{13}C_1$]IAA derived from [$^{13}C_1$]IBA in the lower half-hypocotyl sections and receivers. The level of ester-linked [$^{13}C_1$]IBA was significantly higher than free [$^{13}C_1$]IBA ($P < 0.005$, $n = 3$, Student's t test) in the basipetal group, and the level was not significantly reduced by NPA. IAA eq., IAA equivalents.

we applied 10^{-5} M [$^{13}C_6$]IAA or [$^{13}C_1$]IBA in the donor agar block, a concentration that does not seem to increase auxin conjugation dramatically during a short period of treatment (Sudi, 1966; Venis, 1972) and also yielded detectable amounts of labeled auxins from pooled hypocotyl sections (the amount of transported [$^{13}C_1$]IBA from 20 hypocotyl sections was just above the detection limit). Using Arabidopsis seedlings grown under conditions similar to those used by Rashotte et al. (2003), we found that a significant portion (29%) of the free [$^{13}C_6$]IAA in the hypocotyl sections was transported basipetally, and this basipetal transport was dramatically inhibited by NPA (Fig. 3, A–C). This is consistent with results from assays using [^{3}H]IAA tracers described previously (Liu et al., 2011), and it confirms that transport of IAA plays an important role in regulating the levels of free IAA. In contrast, very little (0.26 pg per plant, less than 1%) free [$^{13}C_1$]IBA was transported, and the amount of transported [$^{13}C_1$]IBA was dramatically lower than the [$^{13}C_6$]IAA (Fig. 3, D–F). This result does not agree with the previous findings, where [^{3}H]IBA was used (Rashotte et al., 2003), suggesting that a large portion of the transported radioactivity in hypocotyls was not [^{3}H]IBA. Interestingly, similar to Rashotte et al. (2003), the transport of [$^{13}C_1$]IBA was not inhibited by NPA (Fig. 3E). Because NPA is an auxin efflux inhibitor (Thomson et al., 1973; Goldsmith, 1982), this result suggests that IBA is not transported by the same efflux proteins that transport IAA. This conclusion is consistent with Ruzicka et al. (2010), who illustrated that the heterologously expressed IAA efflux proteins (PINs and ABCBs) did not use IBA as their substrates, and the heterologously expressed ABCG37 protein displayed substrate specificity for IBA but not IAA. On the other hand, Rashotte et al. (2003) showed that the transport of [^{3}H]IBA was not reduced in Arabidopsis *aux1* mutant roots, and both Yang et al. (2006) and Swarup et al. (2008) showed that 2×10^{-5} M IBA did not competitively inhibit the uptake of 10^{-7} M [^{3}H]IAA by heterologously expressed AUX1 protein, suggesting that the transport influx protein AUX1 recognizes only IAA but not IBA. Swarup et al. (2008) also showed that 2×10^{-5} M IBA reduced the uptake of 10^{-7} M [^{3}H]IAA by heterologously expressed LAX3 protein, but not as effectively as 2×10^{-5} M IAA, suggesting that IBA may be a

substrate for the IAA influx protein LAX3, with a lower affinity than IAA. However, considering that the endogenous level of free IBA is dramatically lower than free IAA (Tognetti et al., 2010), it is not likely that IBA can be transported by LAX3 under physiological conditions. Taken together, our results and previous reports support the conclusion that the mechanisms of IAA and IBA transport are partially, if not completely, distinct.

It is difficult to distinguish the low percentage of [$^{13}C_1$]IBA transported from diffusion or phloem transport. Even though we found that [$^{13}C_1$]IBA transport was not altered in the *nakr1* mutant (Fig. 4), which is defective in some aspects of long-distance phloem transport (Tian et al., 2010), this does not exclude the possibility that [$^{13}C_1$]IBA transport might be reduced in mutants that have defects in other aspects of phloem transport. The Arabidopsis *suc2* mutant, defective in loading Suc into the phloem, could be a candidate for such a test; however, the mutant seedlings are severely dwarfed (Gottwald et al., 2000; Srivastava et al., 2008) and thus are not easily applicable for use in the hypocotyl transport assay (Dr. John Ward, personal communication). Nevertheless, it would be useful to measure IBA transport in mutants that are defective in long-distance phloem transport if the seedlings are either not dramatically stunted or alternative methods can be devised. Such studies could potentially reveal aspects of the mechanism of IBA transport. The low rates of movement we measured, however, are also consistent with a primarily diffusion-mediated mechanism, and the passive diffusion of protonated IBA can be greater than protonated IAA due to the higher hydrophobicity of IBA. On the other hand, basipetal transport of over 60% of the [$^{13}C_1$]IAA derived from [$^{13}C_1$]IBA was detected in the hypocotyl tissues (Fig. 3, G–I), and this transport was significantly inhibited by NPA, suggesting that [$^{13}C_1$]IAA was synthesized from [$^{13}C_1$]IBA before it was transported basipetally in the hypocotyl, and thus the IBA-to-IAA conversion could partially contribute to the transported radioactivity found by Rashotte et al. (2003). (The percentage transport is defined for [$^{13}C_1$]IAA as the amount of [$^{13}C_1$]IAA in the lower section and receiver [0.34 pg; Fig. 3H] divided by the sum of [$^{13}C_1$]IAA in the upper plus lower sections and the receiver [0.54 pg].)

There is an important distinction between the use of radiolabeled auxin measurement of transport and that using stable isotopes and GC-MS. With both procedures, the amount of IAA in the upper hypocotyl section is likely overestimated due to labeled IAA adhering to the plant surfaces; thus, the percentage of transported IAA is potentially underestimated. With stable labels, however, catabolism of IAA or IBA results in compounds, such as oxidized IAA and its conjugates (Ostin et al., 1998; Kai et al., 2007), not detected by the analytical methods used here. Thus, oxidative degradation at the cut hypocotyl surface (Sánchez-Bravo et al., 1988) could result in an underestimate of total transport only when using the radioisotope method (since with [^{3}H]IAA, its catabolites would still be radioactive, localized to the top section, and would contribute to the calculated IAA content). Similarly, catabolism of IAA in the lower section following transport would result in an underestimate of transport by the stable isotope method. The products of IAA and IBA catabolism could potentially be identified by using a modified extraction and derivatization method prior to GC-MS analysis or by using liquid chromatography-MS based methods (Ostin et al., 1998; Tam et al., 2000; Kowalczyk and Sandberg, 2001; Kai et al., 2007), but the stable-labeled standards for each corresponding compound would need to be synthesized for quantification. Nevertheless, we found that the percentage transport of [$^{13}C_1$]IBA-derived [$^{13}C_1$]IAA (Fig. 3I) was twice as much as the percentage transport of [$^{13}C_6$]IAA (Fig. 3C). However, because of these adhesion and metabolic concerns, we cannot be certain that the IBA-derived IAA is preferentially used for polar transport.

Although we could not detect [$^{13}C_6$]IBA derived from [$^{13}C_6$]IAA from five Arabidopsis hypocotyl sections, IAA was previously found to be converted to IBA by enzyme preparations from Arabidopsis seedlings (Ludwig-Müller, 2007). Therefore, the transported [$^{13}C_1$]IBA measured in our assay might also contain [$^{13}C_1$]IBA derived from transported [$^{13}C_1$]IAA. To gain a clearer view of the transport of IBA itself, we analyzed IBA transport in mutants that are defective in the conversions between IAA and IBA (Fig. 1). Because no mutants have been demonstrated to show defects in IAA-to-IBA conversion in vivo, we only analyzed [$^{13}C_1$]IBA transport in the *ibr1 ibr3 ibr10* triple mutant Arabidopsis hypocotyls defective in IBA-to-IAA conversion (Strader et al., 2010; Fig. 5, G–I). We found that [$^{13}C_1$]IBA transport was not altered in the *ibr1 ibr3 ibr10* mutant (Fig. 5, D–F), suggesting that the small amount of transport of IBA does not depend on the interconversion between IBA and IAA. Interestingly, we found that the transport of [$^{13}C_6$]IAA in the *ibr1 ibr3 ibr10* mutant was significantly lower than in the wild type (Fig. 5C). Although we do not know how the IBR proteins might play a role in the transport of IAA, this result could partially explain why the *ibr1 ibr3 ibr10* mutant does not respond to exogenous IAA in a wild-type manner (Strader et al., 2011).

Because both IAA and IBA can be converted to their conjugate forms (Fig. 1), and because the ester-linked IAA conjugate IAA-myoinositol was found to be transported in maize seedlings (Chisnell and Bandurski, 1988), it is also possible that both IAA and IBA conjugates are transported over long distances and thus contributed to the transported radioactivity measured by Rashotte et al. (2003) but were excluded in our assay, where only free IAA and IBA were measured (Figs. 3–5). Therefore, we further quantified the pools of IAA and IBA conjugates using base hydrolysis that selectively breaks ester and amide conjugate bonds. Although the base hydrolysis treatment is relatively harsh, it provides unbiased quantification of the entire IAA and IBA conjugate pools. However, if specific IAA

and IBA conjugates had been of interest, alternative methods using either GC-MS or liquid chromatography-MS could have been applied. As shown in Figure 6B, free [$^{13}C_6$]IAA was the dominant form of transported IAA, and only a very small amount of conjugated [$^{13}C_6$]IAA could be detected after transport. Although our analysis did not include metabolites of [$^{13}C_6$]IAA that do not maintain the indole ring and the two-carbon side chain, this result, together with the percentage of transported free [$^{13}C_6$]IAA (discussed above), leads to the conclusion that IAA itself is the major substrate in the polar transport system. Therefore, transported radioactivity measured in assays with [^{3}H]IAA tracers primarily represents the transport of free IAA in Arabidopsis hypocotyls. However, this does not exclude the possibility that the transport of some IAA conjugates occurs in some plant tissues during some developmental periods to provide free IAA in the target tissue, such as the transport of IAA-myoinositol from the maize kernel to the shoot (Epstein et al., 1980; Nowacki and Bandurski, 1980; Chisnell and Bandurski, 1988). When pools of IBA conjugates were quantified in the lower hypocotyl section and receiver block (Fig. 6D), ester-linked [$^{13}C_1$]IBA was detected at a level significantly higher than free [$^{13}C_1$]IBA, and its level was not affected by NPA applied in the receiver. This result suggests that ester-linked IBA may also be transported basipetally in Arabidopsis hypocotyls and is consistent with what Epstein and Ackerman (1993) found in *Leucadendron discolor*, except that the movement was in a different direction. However, the sum of transported [$^{13}C_1$]IBA and its metabolites analyzed in our assay was still significantly lower than the amount of transported [$^{13}C_6$]IAA, suggesting that the majority of the transported radioactivity derived from [^{3}H]IBA measured by Rashotte et al. (2003) was not from [^{3}H]IBA or [^{3}H]IBA-derived conjugates and [^{3}H]IAA. Therefore, unlike IAA, the measurement of transported radioactivity does not represent the transport of IBA.

Although we found a small amount of transported free and conjugated IBA, the amount is considerably lower than that of IAA, so it is difficult to consider IBA transport as an important means of IBA regulation, in comparison with IAA transport. Because over 29% of the free IAA was transported basipetally (Fig. 3C; discussed above), changes in IAA transport can significantly change the level of free IAA (Liu et al., 2011) and play important roles in root development (Reed et al., 1998; Bhalerao et al., 2002; Salisbury et al., 2007). In contrast, with less than 1% transport of exogenous IBA (Fig. 3I), it is not likely that this transport contributes substantially to the IBA pools at sites distant from where the IBA is applied. In addition, Strader et al. (2011) found that only IAA, but not IBA, could induce lateral root formation in Arabidopsis mutants that were defective in IBA-to-IAA conversion, suggesting that IBA is essentially an auxin precursor rather than active auxin. Because plants have developed a robust and tightly regulated system to transport the active auxin IAA over long distances (for review, see Peer et al., 2011), it may not be necessary to develop another system to continuously transport the auxin precursor IBA similarly over long distances. Additionally, similar to what was suggested by Ruzicka et al. (2010), the transport of IBA may only serve as an additional way to regulate the production of IAA, and the transport may be altered when environmental conditions are changed and IAA production is differently regulated.

The exogenous IAA and IBA were converted to their conjugates in the upper hypocotyl section after the 5-h period (Fig. 6, A and C). IAA formed more amide-linked conjugates than ester-linked conjugates, while IBA was mostly converted to ester-linked conjugates. Interestingly, the level of amide-linked [$^{13}C_6$]IAA in the upper section was significantly increased when NPA was added in the receiver block, while the level of free [$^{13}C_6$]IAA was not changed (Fig. 6A). Because the transport of [$^{13}C_6$]IAA into the lower section was significantly inhibited by NPA (Fig. 6B), and thus [$^{13}C_6$]IAA could accumulate in the upper section, this result suggests that conjugating IAA via amide linkages might be a way to regulate the level of free IAA by removing the excess amount of IAA, and at least for the amide-linked IAA conjugates IAA-Asp and IAA-Glu, they may be further metabolized by oxidative degradation (Tuominen et al., 1994).

The formation of the large amount of ester-linked IBA is consistent with what was found previously, and the major conjugate is most likely IBA-Glc (Epstein and Ackerman, 1993; Ludwig-Müller and Epstein, 1993; Baraldi et al., 1995). On the other hand, the total amount of free and conjugated [$^{13}C_1$]IBA in the upper section was dramatically higher than the amount of total [$^{13}C_6$]IAA, suggesting that the uptake of [$^{13}C_1$]IBA through the cut surface was greater than that for [$^{13}C_6$]IAA. However, it was found that the uptake of [^{3}H]IBA was the same as the uptake of [^{3}H]IAA in intact Arabidopsis seedlings (Ludwig-Müller et al., 1995b). We also analyzed the stability of [$^{13}C_1$]IBA and [$^{13}C_6$]IAA in the donor agar block and found that the same proportion (65%) of [$^{13}C_1$]IBA and [$^{13}C_6$]IAA remained in the donor agar block after the 5-h transport period, suggesting that the higher uptake of [$^{13}C_1$]IBA is not due to a higher stability of [$^{13}C_1$]IBA in the donor agar block. Because Tognetti et al. (2010) found that the gene encoding the IBA-Glc-conjugating enzyme (*UGT74E2*) was rapidly and strongly induced by oxidative stress and the level of IBA-Glc was dramatically increased under stress conditions, it is possible that the IBA-Glc-conjugating activity was significantly induced at the cut surface of the hypocotyl and that the formation of IBA-Glc conjugates led to more IBA taken up into the plant tissue. This finding can also be linked to the phenomenon that IBA is better than IAA in stimulating adventitious root formation in plant cuttings, possibly because plant tissues store more exogenous IBA than IAA in a conjugate form, which can release free IBA over a long period of time after the application of exogenous IBA (Epstein et al., 1993) and eventually provide free IAA for root primordia induction (Liu and Reid, 1992).

In summary, we evaluated the transport of IAA and IBA in Arabidopsis hypocotyls using stable isotope-labeled tracers and GC-MS/MS. We found that, in contrast to previous reports using radioactive assays, the transport of free IBA was much lower than the transport of free IAA and was not inhibited by NPA, and that IBA was metabolized to IAA and IBA conjugates during the transport while IAA remained as free IAA after transport. We conclude that the mechanism of IBA transport is fundamentally different from IAA, and the transport and metabolism of IBA can be an additional means to regulate the levels of free IAA that can trigger physiological responses.

Our study also shows that by using stable isotope labeling and MS, the movement and metabolism of both endogenous and applied compounds in plants can be accurately identified and quantified. Therefore, in addition to an analysis of auxin transport and metabolism, we have also demonstrated a model system that should prove useful for the analysis of the transport and metabolism of other plant hormones and small molecules that have potential regulatory activity.

MATERIALS AND METHODS

Plant Materials and Growth Conditions

Wild-type Arabidopsis (*Arabidopsis thaliana*) and *ibr1 ibr3 ibr10* seeds were gifts from Dr. Bonnie Bartel, and *nakr1* seeds were from Dr. John Ward. All experiments were performed with ecotype Columbia. Seeds were imbibed in distilled water for a few hours, surface sterilized in 2.0-mL microcentrifuge tubes with 1 mL of 70% ethanol for 2 min followed by 1 mL of 30% commercial bleach (to yield 2% sodium hypochlorite) for 5 min, and washed with sterile water five times. Seeds were sown onto MS medium (4.33 g L^{-1} Murashige and Skoog salts; MSP01-50LT; Caisson Labs), 0.8% (w/v) Phytoblend agar (PTP01-500GM; Caisson Labs), and 1.5% (w/v) Suc (Sigma-Aldrich), pH 5.7. After seeding, agar plates were wrapped with Parafilm (Pechiney Plastic Packaging) and kept at 4°C for 3 d, and seedlings were grown vertically on the plates at room temperature (22°C) under 5 μmol m^{-2} (photosynthetically active radiation) continuous cool-white fluorescent light for 5 d before the measurement of auxin transport. These growth conditions were similar to those described by Rashotte et al. (2003).

Synthesis of Stable Isotope-Labeled IBA

The synthesis of [$^{13}C_8$,$^{15}N_1$]IBA was as described previously (Cohen and Schulze, 1981; Barkawi et al., 2008). The same synthesis and purification methods were used to synthesize [$^{13}C_1$]IBA, using [2-^{13}C]indole (CLM-1863; Cambridge Isotope Laboratories) as the starting material for synthesis. The concentration of the [$^{13}C_1$]IBA product was determined by UVA_{282} (ε = 6,060) and confirmed by reverse-isotope dilution selected ion monitoring GC-MS with an unlabeled IBA standard.

Hypocotyl Auxin Transport Assays

The hypocotyl basipetal IAA transport assay was modified from that recently described (Liu et al., 2011). Six millimeters of an Arabidopsis hypocotyl section harvested directly below the shoot apex was placed on an agar plate after excision, and an auxin donor block of 1.5% agar (Sigma-Aldrich) containing 0.2 M MES (Sigma-Aldrich) and 10^{-5} M [$^{13}C_6$]IAA (CLM-1896; Cambridge Isotope Laboratories) or 10^{-5} M [$^{13}C_1$]IBA was placed in contact with the apical end of the tissue section, while a receiver agar block containing 0.2 M MES (pH 6.5) was placed in contact with the basal end. Receiver blocks containing 0.2 M MES (pH 6.5) and 10^{-5} M NPA (ChemService) were used as the +NPA control, and a second control was used in which the orientation of the tissue section was inverted (acropetal control). Two strips of polyethylene film (Saran Original; S.C. Johnson & Sons) were placed between the agar blocks and the support agar on the plates to avoid diffusion of stable-labeled auxin through the support agar and thus prevent an undesirable increase in background. The agar plates were placed vertically with donor blocks down for 5 h in a chamber with high humidity provided by moist filter paper, and each hypocotyl section was then divided into apical and basal halves. When [$^{13}C_6$]IAA was added in the donor blocks, five replicates of basal half-hypocotyl sections and receiver blocks were pooled into one microcentrifuge tube, and the corresponding apical half-hypocotyl sections were pooled into another microcentrifuge tube. Samples were collected in a similar way when [$^{13}C_1$]IBA was added in the donor blocks, but 20 replicates of hypocotyl sections were pooled into one microcentrifuge tube. The samples were frozen in liquid nitrogen quickly after collection and stored in a −80°C freezer before quantification of free stable-labeled auxins. When conjugated stable-labeled auxins were quantified, sample sizes were doubled and twice the number of tissue sections were pooled into one sample.

Quantification of Free Stable Isotope-Labeled IAA and IBA

The quantification methods were modified from methods described previously (Barkawi et al., 2010; Liu et al., 2011). For samples that were treated with [$^{13}C_6$]IAA in the donor block, 20 μL of homogenization buffer (35% 0.2 M imidazole, 65% isopropanol, pH 7) containing 0.2 ng of [$^2H_4$]IAA (a gift from Prof. R.S. Bandurski; Magnus et al., 1980) and 0.2 ng of [$^{13}C_8$,$^{15}N_1$]IBA was added; for samples that were treated with [$^{13}C_1$]IBA, 40 μL of homogenization buffer containing 0.2 ng of [$^2H_4$]IAA and 0.2 ng of [$^{13}C_8$,$^{15}N_1$]IBA was added. Tissues were homogenized using a Mixer Mill (MM 300; Qiagen) with tungsten carbide beads (3-mm beads for 1.5-mL tubes and 2.3-mm beads for 0.5-mL tubes; Craig Ball Sales). After 1 h on ice, the homogenate was diluted 10 times by adding water and then centrifuged at 10,000*g* for 10 min. The supernatant was passed through a 200-μL TopTips (TT2EMT.96; Glygen) solid-phase extraction column containing 5 mg of NH_2 anion-exchange resin (12213020; Varian) and then washed by a series of solvents and solutions essentially as described by Liu et al. (2011). To reduce the loss of IBA during extraction, only 60 μL each of hexane and methanol was used to wash the resin after diluted plant homogenate was loaded. IAA and IBA were both eluted from the solid-phase extraction tip by 3 × 80 μL of 0.25% phosphoric acid (A242; Fisher Chemicals), and the eluate was partitioned against 100 μL of ethyl acetate (E195-4; Fisher Chemicals). The ethyl acetate layer was collected and transferred to a 250-μL glass insert (CTI-9425; ChromTech), and the sample was methylated in the insert by adding ethereal diazomethane in the presence of 10% methanol (34860; Sigma-Aldrich) and waiting 5 min; then, the solvents were evaporated under a stream of N_2 gas, and the sample was redissolved in 15 μL of ethyl acetate. The methylated IAA and IBA were analyzed using GC-selected reaction monitoring (SRM)-MS on a Thermo Trace GC Ultra device coupled to a TSQ Vantage triple quadrupole MS system (Thermo Scientific) under the conditions described previously (Barkawi et al., 2010; Liu et al., 2011). The quinolinium ions produced from the molecular ions of IAA (Fig. 2B; mass-to-charge ratio [*m/z*] 130 from *m/z* 189, *m/z* 131 from *m/z* 190, *m/z* 134 from *m/z* 193, and *m/z* 136 from *m/z* 195) were selected by the third quadrupole and monitored for the first 10.5 min of the chromatographic run. The quinolinium ions produced from the molecular ions of IBA (Fig. 2C; *m/z* 130 from *m/z* 217, *m/z* 131 from *m/z* 218, *m/z* 136 from *m/z* 223, and *m/z* 139 from *m/z* 226) were selected and monitored starting at 10.5 min until the end of the run. Levels of [$^{13}C_6$]IAA or [$^{13}C_1$]IAA derived from [$^{13}C_1$]IBA were quantified by isotope dilution analysis based on the [$^2H_4$]IAA internal standard; levels of [$^{13}C_1$]IBA were quantified by isotope dilution analysis based on the [$^{13}C_8$,$^{15}N_1$] IBA internal standard. The natural abundance of ^{13}C was determined using unlabeled chemical standards (Sigma) and is corrected for in the calculations and the data reported.

Quantification of [$^{13}C_6$]IAA and [$^{13}C_1$]IBA in Donor Agar Blocks

Donor agar blocks containing 10^{-5} M [$^{13}C_6$]IAA and 10^{-5} M [$^{13}C_1$]IBA were placed on top of the apical end of Arabidopsis hypocotyl sections as described above. The agar blocks were collected into microcentrifuge tubes after 0- and 5-h transport periods, and the tubes were weighed and quickly frozen in liquid N_2. The agar blocks were homogenized using the Mixer Mill as described above, after adding 400 μL of methanol containing 10 μL each of 10^{-5} M IAA and 10^{-5} M [$^{13}C_8$,$^{15}N_1$]IBA as the internal standards. After 1 h of

incubation on ice, 100 μL of supernatant from the homogenate was transferred into a 2-mL glass vial and methylated by ethereal diazomethane. The methylated samples were dried under a stream of N_2 gas, resuspended in 20 μL of ethyl acetate, and analyzed by GC-MS. The amounts of [$^{13}C_6$]IAA and [$^{13}C_1$]IBA present per milligram of the donor agar block were calculated based on the internal standards and the weight of the agar block. Finally, the percentage of [$^{13}C_6$]IAA and [$^{13}C_1$]IBA remaining in the 5-h samples (divided by the initial 0-h time point) was determined.

Quantification of Ester-Linked and Amide-Linked [$^{13}C_6$]IAA and [$^{13}C_1$]IBA

For samples that were treated with [$^{13}C_6$]IAA in the donor block, 40 μL of homogenization buffer containing 0.6 ng of [$^2H_4$]IAA and 0.6 ng of [$^{13}C_8$,$^{15}N_1$]IBA was added. After homogenization and 1 h on ice as described above, 20 μL of the homogenate was used for the quantification of free [$^{13}C_6$]IAA as described above. Of the remainder of the homogenate, 15 μL was hydrolyzed in 1 N NaOH (1 h, room temperature) for measurement of free plus ester-linked [$^{13}C_6$]IAA, and 10 μL was hydrolyzed in 7 N NaOH (3 h, 100°C under N_2) for measurement of total [$^{13}C_6$]IAA (free plus ester-linked and amide-linked [$^{13}C_6$]IAA). Extraction and methylation of free IAA plus that released from the conjugates were as described previously (Liu et al., 2011), and the method for GC-SRM-MS analysis was as described above. Levels of free [$^{13}C_6$]IAA, free plus ester-linked [$^{13}C_6$]IAA, and total [$^{13}C_6$]IAA were quantified by isotope dilution analysis based on the [$^2H_4$]IAA internal standard, as described above. The results were displayed as picogram IAA equivalents, since the chemical structures of every conjugate formed are not known.

For samples that were treated with [$^{13}C_1$]IBA in the donor block, 80 μL of homogenization buffer containing 0.6 ng of [$^2H_4$]IAA and 0.6 ng of [$^{13}C_8$,$^{15}N_1$]IBA was added, and the homogenate was divided into three parts: 40 μL was used for the quantitation of free [$^{13}C_1$]IBA and [$^{13}C_1$]IAA derived from the [$^{13}C_1$]IBA; 30 μL was used for the measurement of free plus ester-linked [$^{13}C_1$]IBA; and 10 μL was used for the measurement of total [$^{13}C_1$]IBA. Hydrolysis, extraction, methylation, GC-SRM-MS analysis, and quantification of free and conjugated [$^{13}C_1$]IBA were as described above.

Arabidopsis Genome Initiative locus identifiers for genes mentioned in this article are as follows: IBR1, At4g05530; IBR3, At3g06810; IBR10, At4g14430; and NaKR1, At5g02600.

Supplemental Data

The following materials are available in the online version of this article.

Supplemental Figure S1. Transport of free [$^{13}C_8$,$^{15}N_1$]IBA and [$^{13}C_8$,$^{15}N_1$]IAA derived from [$^{13}C_8$,$^{15}N_1$]IBA in maize coleoptiles after 3.5-h transport periods.

ACKNOWLEDGMENTS

We thank Dr. Bonnie Bartel (Rice University) for wild-type and *ibr1 ibr3 ibr10* seeds and Dr. John Ward (University of Minnesota) for the seeds of the *nakr1* mutant and comments on the selection of phloem transport mutants. We thank Dr. Robert S. Bandurski (Michigan State University) for the gift of [$^2H_4$]IAA that was synthesized in his laboratory by Dr. Volker Magnus (deceased). We also thank Dr. Jane Glazebrook (University of Minnesota) for critical reading of the manuscript.

Received November 17, 2011; accepted February 9, 2012; published February 9, 2012.

LITERATURE CITED

Baldi BG, Maher BR, Cohen JD (1989) Hydrolysis of indole-3-acetic acid esters exposed to mild alkaline conditions. Plant Physiol **91:** 9–12

Baraldi R, Bertazza G, Bregoli A, Fasolo F, Rotondi A, Predieri S, Serafini-Fracassini D, Slovin JP, Cohen JD (1995) Auxins and polyamines in relation to differential *in vitro* root induction on microcuttings of two pear cultivars. J Plant Growth Regul **14:** 49–59

Barkawi LS, Tam Y-Y, Tillman JA, Normanly J, Cohen JD (2010) A high-throughput method for the quantitative analysis of auxins. Nat Protoc **5:** 1609–1618

Barkawi LS, Tam YY, Tillman JA, Pederson B, Calio J, Al-Amier H, Emerick M, Normanly J, Cohen JD (2008) A high-throughput method for the quantitative analysis of indole-3-acetic acid and other auxins from plant tissue. Anal Biochem **372:** 177–188

Bhalerao RP, Eklöf J, Ljung K, Marchant A, Bennett M, Sandberg G (2002) Shoot-derived auxin is essential for early lateral root emergence in Arabidopsis seedlings. Plant J **29:** 325–332

Bialek K, Cohen JD (1989) Quantitation of indoleacetic acid conjugates in bean seeds by direct tissue hydrolysis. Plant Physiol **90:** 398–400

Chisnell JR, Bandurski RS (1988) Translocation of radiolabeled indole-3-acetic acid and indole-3-acetyl-*myo*-inositol from kernel to shoot of *Zea mays* L. Plant Physiol **86:** 79–84

Cohen JD, Schulze A (1981) Double-standard isotope dilution assay. I. Quantitative assay of indole-3-acetic acid. Anal Biochem **112:** 249–257

Epstein E, Ackerman A (1993) Transport and metabolism of indole-3-butyric acid in cuttings of *Leucadendron discolor*. Plant Growth Regul **12:** 17–22

Epstein E, Cohen JD, Bandurski RS (1980) Concentration and metabolic turnover of indoles in germinating kernels of *Zea mays* L. Plant Physiol **65:** 415–421

Epstein E, Sagee O (1992) Effect of ethylene treatment on transport and metabolism of indole-3-butyric acid in citrus leaf midribs. Plant Growth Regul **11:** 357–362

Epstein E, Zilkah S, Faingersh G, Rotebaum A (1993) Transport and metabolism of indole-3-butyric acid in easy- and difficult-to-root cuttings of sweet cherry (*Prunus avium* L.). Acta Hortic **329:** 292–295

Goldsmith MHM (1982) A saturable site responsible for polar transport of indole-3-acetic acid in sections of maize coleoptiles. Planta **155:** 68–75

Gottwald JR, Krysan PJ, Young JC, Evert RF, Sussman MR (2000) Genetic evidence for the in planta role of phloem-specific plasma membrane sucrose transporters. Proc Natl Acad Sci USA **97:** 13979–13984

Kai K, Horita J, Wakasa K, Miyagawa H (2007) Three oxidative metabolites of indole-3-acetic acid from Arabidopsis thaliana. Phytochemistry **68:** 1651–1663

Kowalczyk M, Sandberg G (2001) Quantitative analysis of indole-3-acetic acid metabolites in Arabidopsis. Plant Physiol **127:** 1845–1853

Li Y, Wu YH, Hagen G, Guilfoyle T (1999) Expression of the auxin-inducible GH3 promoter/GUS fusion gene as a useful molecular marker for auxin physiology. Plant Cell Physiol **40:** 675–682

Liu J-H, Reid DM (1992) Adventitious rooting in hypocotyls of sunflower (*Helianthus annuus*) seedlings. IV. The role of changes in endogenous free and conjugated indole-3-acetic acid. Physiol Plant **86:** 285–292

Liu X, Cohen JD, Gardner G (2011) Low-fluence red light increases the transport and biosynthesis of auxin. Plant Physiol **157:** 891–904

Ludwig-Müller J (2000) Indole-3-butyric acid in plant growth and development. Plant Growth Regul **32:** 219–230

Ludwig-Müller J (2007) Indole-3-butyric acid synthesis in ecotypes and mutants of *Arabidopsis thaliana* under different growth conditions. J Plant Physiol **164:** 47–59

Ludwig-Müller J, Epstein E (1993) Indole-3-butyric acid in *Arabidopsis thaliana*. II. *In vivo* metabolism. Plant Growth Regul **13:** 189–195

Ludwig-Müller J, Hilgenberg W, Epstein E (1995a) The *in vitro* biosynthesis of indole-3-butyric acid in maize. Phytochemistry **40:** 61–68

Ludwig-Müller J, Raisig A, Hilgenberg W (1995b) Uptake and transport of indole-3-butyric acid in *Arabidopsis thaliana*: comparison with other natural and synthetic auxins. J Plant Physiol **147:** 351–354

Ludwig-Müller J, Sass S, Sutter E, Wodner M, Epstein E (1993) Indole-3-butyric acid in *Arabidopsis thaliana*. I. Identification and quantification. Plant Growth Regul **13:** 179–187

Magnus V, Bandurski RS, Schulze A (1980) Synthesis of 4,5,6,7 and 2,4,5,6,7 deuterium-labeled indole-3-acetic acid for use in mass spectrometric assays. Plant Physiol **66:** 775–781

Marx M, Djerassi C (1968) Mass spectrometry in structural and stereochemical problems. CXLIX. The question of ring expansion in the fragmentation of ^{13}C-labeled nitrogen heterocycles. J Am Chem Soc **90:** 678–681

Nowacki J, Bandurski RS (1980) *Myo*-inositol esters of indole-3-acetic acid as seed auxin precursors of *Zea mays* L. Plant Physiol **65:** 422–427

Ostin A, Kowalyczk M, Bhalerao RP, Sandberg G (1998) Metabolism of indole-3-acetic acid in *Arabidopsis*. Plant Physiol **118:** 285–296

Peer WA, Blakeslee JJ, Yang H, Murphy AS (2011) Seven things we think we know about auxin transport. Mol Plant **4:** 487–504

Rashotte AM, Poupart J, Waddell CS, Muday GK (2003) Transport of the

two natural auxins, indole-3-butyric acid and indole-3-acetic acid, in Arabidopsis. Plant Physiol **133:** 761–772

Reed RC, Brady SR, Muday GK (1998) Inhibition of auxin movement from the shoot into the root inhibits lateral root development in Arabidopsis. Plant Physiol **118:** 1369–1378

Ruzicka K, Strader LC, Bailly A, Yang H, Blakeslee J, Langowski L, Nejedlá E, Fujita H, Itoh H, Syono K, et al (2010) Arabidopsis PIS1 encodes the ABCG37 transporter of auxinic compounds including the auxin precursor indole-3-butyric acid. Proc Natl Acad Sci USA **107:** 10749–10753

Salisbury FJ, Hall A, Grierson CS, Halliday KJ (2007) Phytochrome coordinates Arabidopsis shoot and root development. Plant J **50:** 429–438

Sánchez-Bravo J, Ortuño A, Acosta M, Sabater F (1988) *In vivo* metabolism of labeled indole-3-acetic acid during polar transport in etiolated hypocotyls of *Lupinus albus*: relationship with growth. Plant Growth Regul **7:** 271–288

Seidel C, Walz A, Park S, Cohen JD, Ludwig-Müller J (2006) Indole-3-acetic acid protein conjugates: novel players in auxin homeostasis. Plant Biol (Stuttg) **8:** 340–345

Slovin JP, Bandurski RS, Cohen JD (1999) Auxin. *In* P Hooykaas, M Hall, K Libbenga, eds, Biochemistry and Molecular Biology of Plant Hormones. Elsevier, Amsterdam, pp 115–140

Srivastava AC, Ganesan S, Ismail IO, Ayre BG (2008) Functional characterization of the Arabidopsis AtSUC2 sucrose/H^+ symporter by tissue-specific complementation reveals an essential role in phloem loading but not in long-distance transport. Plant Physiol **148:** 200–211

Staswick PE, Serban B, Rowe M, Tiryaki I, Maldonado MT, Maldonado MC, Suza W (2005) Characterization of an *Arabidopsis* enzyme family that conjugates amino acids to indole-3-acetic acid. Plant Cell **17:** 616–627

Strader LC, Bartel B (2011) Transport and metabolism of the endogenous auxin precursor indole-3-butyric acid. Mol Plant **4:** 477–486

Strader LC, Culler AH, Cohen JD, Bartel B (2010) Conversion of endogenous indole-3-butyric acid to indole-3-acetic acid drives cell expansion in Arabidopsis seedlings. Plant Physiol **153:** 1577–1586

Strader LC, Wheeler DL, Christensen SE, Berens JC, Cohen JD, Rampey RA, Bartel B (2011) Multiple facets of *Arabidopsis* seedling development require indole-3-butyric acid-derived auxin. Plant Cell **23:** 984–999

Sudi J (1966) Increases in the capacity of pea tissue to form acyl-aspartic acids specifically induced by auxins. New Phytol **65:** 9–21

Sutter EG, Cohen JD (1992) Measurement of indolebutyric acid in plant tissues by isotope dilution gas chromatography-mass spectrometry analysis. Plant Physiol **99:** 1719–1722

Swarup K, Benková E, Swarup R, Casimiro I, Péret B, Yang Y, Parry G, Nielsen E, De Smet I, Vanneste S, et al (2008) The auxin influx carrier LAX3 promotes lateral root emergence. Nat Cell Biol **10:** 946–954

Tam YY, Epstein E, Normanly J (2000) Characterization of auxin conjugates in Arabidopsis: low steady-state levels of indole-3-acetyl-aspartate, indole-3-acetyl-glutamate, and indole-3-acetyl-glucose. Plant Physiol **123:** 589–596

Thomson K-S, Hertel R, Müller S, Tavares JE (1973) 1-N-Naphthylphthalamic acid and 2,3,5-triiodobenzoic acid. Planta **109:** 337–352

Tian H, Baxter IR, Lahner B, Reinders A, Salt DE, Ward JM (2010) *Arabidopsis* NPCC6/NaKR1 is a phloem mobile metal binding protein necessary for phloem function and root meristem maintenance. Plant Cell **22:** 3963–3979

Tognetti VB, Van Aken O, Morreel K, Vandenbroucke K, van de Cotte B, De Clercq I, Chiwocha S, Fenske R, Prinsen E, Boerjan W, et al (2010) Perturbation of indole-3-butyric acid homeostasis by the UDP-glucosyltransferase *UGT74E2* modulates *Arabidopsis* architecture and water stress tolerance. Plant Cell **22:** 2660–2679

Tuominen H, Ostin A, Sandberg G, Sundberg B (1994) A novel metabolic pathway for indole-3-acetic acid in apical shoots of *Populus tremula* (L.) × *Populus tremuloides* (Michx.). Plant Physiol **106:** 1511–1520

Venis MA (1972) Auxin-induced conjugation systems in peas. Plant Physiol **49:** 24–27

Went F, White R (1938) Experiments of the transport of auxin. Bot Gaz **100:** 465–484

Woodward AW, Bartel B (2005) Auxin: regulation, action, and interaction. Ann Bot (Lond) **95:** 707–735

Yang T, Davies P (1999) Promotion of stem elongation by indole-3-butyric acid in intact plants of *Pisum sativum* L. Plant Growth Regul **27:** 157–160

Yang Y, Hammes UZ, Taylor CG, Schachtman DP, Nielsen E (2006) High-affinity auxin transport by the AUX1 influx carrier protein. Curr Biol **16:** 1123–1127